JOURNAL OF VIROLOGY, Dec. 1996, p. 8391–8401 Vol. 70, No. 12
0022-538X/96/$04.00+0

Effect of M1 Protein and Low pH on Nuclear Transport of Influenza Virus Ribonucleoproteins

MATTHEW BUI, GARY WHITTAKER, AND ARI HELENIUS*
Yale University School of Medicine, New Haven, Connecticut 06510

Received 7 June 1996/Accepted 27 August 1996

Influenza virus enters its host cell by receptor-mediated endocytosis followed by acid-activated membrane fusion in endosomes. The viral ribonucleoprotein particles (vRNPs) delivered into the cytosol then dissociate from the matrix protein, M1, and from each other, after which they are individually imported into the nucleus via the nuclear pores. For some time, it has been believed that the low pH in endosomes may, in some way, trigger the capsid disassembly events necessary for nuclear transport. This report provides direct evidence that the association of M1 with vRNPs is sensitive to mildly acidic pH within the infected cell. Recombinant M1, expressed in cultured cells, was found to associate with vRNPs and inhibit their nuclear import. Brief acidification of the cytosolic compartment eliminated the interfering activity and allowed the incoming vRNPs to enter the nucleus. Newly assembled progeny M1-vRNP complexes in the cytosol of infected cells were also dissociated by brief acidification. Acidic pH was thus found to serve as a switch that allowed M1 to carry out its multiple functions in the uncoating, nuclear transport, and assembly of vRNPs.

Among RNA viruses, influenza virus is unusual in that it replicates in the nucleus. During virus entry the genome and accessory proteins are efficiently imported into the nucleus in the form of viral ribonucleoprotein (vRNPs). Later in infection, the newly synthesized progeny vRNPs are exported from the nucleus to the cytosol. Virus morphogenesis occurs at the plasma membrane. The bidirectional nuclear transport of vRNPs occurs via the nuclear pore complexes and is regulated by the expression of other viral proteins, notably M1, the membrane (matrix) protein (25).

Since the genome is segmented, traffic into and out of the nucleus occurs in the form of eight individually assembled vRNPs (for reviews, see references 12, 18, and 54). These are helical structures composed of a negative-sense RNA molecule and numerous copies of a nucleoprotein (56 kDa; one per approximately 20 nucleotides) (3, 6, 13). The three polymerase subunits, PA, PB1, and PB2, form a heterotrimer located at one end of the elongated vRNP complex (29). The viral matrix protein (M1, 27 kDa), the most abundant of the proteins in the virus particle, associates tightly with the vRNPs both in the virion and also during virus assembly within the infected cell (37, 59).

The stepwise entry of influenza virus into cells has been studied extensively. After binding to sialic acid-containing receptors on the cell surface, viruses are internalized by receptor-mediated endocytosis (28). Penetration occurs in late endosomes and is triggered by an activation of the viral membrane fusion factors, the hemagglutinin (HA) spikes, at approximate pH values of 5.5 (23, 52). The acid-triggered fusion can be prevented by carboxylic ionophores, acidotropic agents that raise the pH in endosomes (24), and by inhibitors that block the vacuolar proton pumps that maintain the low endosomal pH (8). After nucleocapsids are delivered into the cytosol, they dissociate into their component vRNPs and release the M1. The vRNPs are rapidly and efficiently imported into the nucleus through the nuclear pore complexes by an active process (26).

Mounting evidence suggests that the interaction with M1 determines whether vRNPs are transported into or out of the nucleus. Our earlier results have shown that association with M1 is needed for vRNP export from the nucleus (25, 53). They have also strongly suggested that M1 dissociation is necessary for nuclear import. Amantadine and rimantadine, two anti-influenza virus drugs, have been shown to prevent M1 dissociation from vRNPs during virus entry and inhibit vRNP transport into the nucleus (2, 25). Since the antiviral effect of these drugs is caused by inhibiting the acid-activated cation channel, M2, in the viral envelope (11, 35, 45, 47, 51), the M2 ion channel activity is thought to permit the flow of ions into the viral interior to cause nucleocapsid dissociation (reviewed in reference 12). It has also been reported that low pH induces M1 dissociation from vRNPs of purified viruses in vitro (57, 58). It was therefore hypothesized that the dissociation of M1 from vRNPs is caused by exposure of the viral nucleocapsid to the low pH in the endosomes (25, 27). The evidence in support of this hypothesis has, however, remained largely conjectural.

At late stages of infection, M1 must reassociate with vRNPs for virus assembly. M1 associates tightly with vRNPs to constitute a stable nucleocapsid complex (3, 6, 48, 56). These M1-vRNP complexes are then incorporated into a mature virus particle by budding at the plasma membrane. By ultrastructural examination, M1 is localized on the interior side of the viral membrane bilayer, forming a shell which surrounds the nucleocapsid (34, 42). The lipid and RNA binding properties of M1 support the concept that M1 may serve as a bridge between the vRNPs and the viral membrane (48, 56).

In this study, we have focused on the role of the M1-vRNP interactions during virus entry into and assembly in live cells. The results provide direct evidence both for the role of M1 as a master regulator of vRNP transport through the nuclear membrane and for the direct involvement of low pH in modulating the activity of M1, allowing it to carry out multiple functions within the virus life cycle.

* Corresponding author. Mailing address: Department of Cell Biology, School of Medicine, Sterling Hall of Medicine, P.O. Box 208002, New Haven, CT 06520-8002. Phone: (203) 785-4313. Fax: (203) 785-7446. Electronic mail address: ARI_HELENIUS@QM.YALE.EDU.

MATERIALS AND METHODS

Cells and viruses. Chinese hamster ovary (CHO) cells and L929 cells were grown as monolayers and passaged biweekly in α minimal essential medium supplemented with 8% fetal calf serum (FCS), glutamine, and penicillin-strep-

tomycin (100 U/ml [each]). L929 cells have been reported to undergo abortive infections with some influenza virus strains, but synthesis of virus proteins was normal and infectious virus was produced for the WSN strain used here (53). Madin-Darby bovine kidney (MDBK) cells were grown as monolayers and passaged biweekly in Dulbecco's minimal essential medium (DMEM) supplemented with 7% FCS, glutamine, and penicillin-streptomycin. HeLa cells were also passaged biweekly and grown in MEM supplemented with 7% FCS, glutamine, and penicillin-streptomycin. The 3PNP-4 cell line (20) constitutively expresses NP and the polymerases and was a gift from Mark Krystal (Bristol Myers Squibb, Wallingford, Conn.). 3PNP-4 cells were passaged biweekly and grown in αMEM supplemented with 10% FCS, glutamine, and 400 μg of Geneticin per ml (Gibco).

The WSN strain of influenza A virus was obtained from the laboratory of Robert Krug (Rutgers University). WSN virus stocks were grown, and their titers were determined by plaque assay in MDBK cells at 37°C as described previously (26). WSN virus labeled with [^{35}S]methionine and [^{35}S]cysteine was prepared as described previously (26). Semliki Forest virus (SFV) was grown and its titer was determined in BHK-21 cells as previously described (44).

The recombinant SFV expressing M1 was constructed in the following way. The M1 gene from WSN was obtained from Peter Palese (Mount Sinai University) and cloned into the pSFV vector, obtained from Henrik Garoff (Karolinska Institute). SP6 polymerase was used to synthesize mRNAs from pSFV-M1 plasmid and pHelper plasmid, which encodes the structural proteins (also a gift from Henrik Garoff). Both mRNAs were electroporated simultaneously into 10^6 BHK cells in 0.8 ml of phosphate-buffered saline (PBS) without calcium or magnesium. The Bio-Rad Gene Pulser apparatus was set at 960 V and 25 μF capacitance, and the cuvette used had a 0.4-cm gap. Cells were plated and incubated at 37°C for 36 h, after which the supernatant was collected into aliquots and stored at −70°C for use as recombinant virus stocks. Since the viruses obtained were limited to a single round of infection, virus titers were assessed by immunofluorescence microscopy with an antibody against the M1 protein.

The SFV-lacZ recombinant virus which expresses β-galactosidase was prepared in the same manner described above for the SFV-M1 virus. The pSFV-lacZ plasmid was obtained from Henrik Garoff.

Antibodies. Polyclonal antibodies against whole WSN virus were prepared by immunizing rabbits with detergent-treated and UV-irradiated purified virus (26). Polyclonal antiserum to M1 was prepared by immunizing rabbits with gel-purified protein (26). Hybridomas that secrete monoclonal antibodies against WSN viral proteins NP (46/4 and M2-1C64R3) were purchased from the American Type Culture Collection and used to prepare hybridoma supernatants. An affinity-purified monoclonal antibody against β-galactosidase was a gift from Jack Rose (Yale University).

Virus infection. Virus diluted in binding medium (RPMI 1640 without sodium bicarbonate and supplemented with 0.2% bovine serum albumin (BSA) and 10 mM *N*-2-hydroxyethylpiperazine-*N*′-2-ethanesulfonic acid [HEPES; pH 6.8]) was bound to cells for 90 min at 4°C. The cells were then washed with cold RPMI 1640 medium to remove unbound virus. To initiate infection, medium at 37°C (supplemented with FCS and containing sodium bicarbonate) was added, and the bound virus was allowed to internalize at 37°C in a CO_2 incubator. Time postinfection was calculated as time at 37°C. In experiments to examine incoming vRNPs, cells were infected at high multiplicity of infection (MOI), approximately 150 to 200 PFU per cell, and cycloheximide (1 mM) was included to prevent the synthesis of viral proteins. This concentration of cycloheximide was determined to block viral protein synthesis completely without affecting the nuclear import of vRNPs. In certain control samples, medium containing 25 mM NH_4Cl buffered to pH 7.5 was added during viral entry to raise the endosomal pH (31) and thus inhibit viral fusion and penetration.

Indirect immunofluorescence microscopy. Immunofluorescence microscopy was carried out essentially as described previously (26). Briefly, cells were fixed with 3% paraformaldehyde in PBS for 15 min, quenched with 50 mM NH_4Cl–PBS, and permeabilized for 5 min with 0.1% Triton X-100–PBS. After blocking in 10% goat serum, cells were incubated with primary and secondary antibodies for 30 min each and mounted in Mowiol with 2.5% 1,4-diazabicyclo[2.2.2]octane (DABCO) to prevent photo bleaching. The antibodies used were a pool of anti-NP monoclonal antibodies or a monospecific anti-M1 polyclonal antibody, 7648. As secondary antibodies, we used Texas Red-labeled goat anti-rabbit immunoglobulin G, and fluorescein isothiocyanate-labeled goat anti-mouse immunoglobulin G (Zymed). Cells were viewed with a Zeiss Axiophot microscope fitted with a 40× objective lens, and images were photographed with TMAX 400 film (Kodak).

Microinjection of vRNPs. vRNPs were prepared by procedures described previously (16). Briefly, purified WSN virus (1 mg of protein) was diluted with 4 volumes of 10% (wt/vol) sucrose–MNT [25 mM Tris, 25 mM 2-(*N*-morpholino) ethanesulfonic acid (MES), 150 mM NaCl (pH 7.5)] and pelleted by centrifugation at 35,000 rpm in an SW 50.1 rotor for 40 min at 4°C. The virus pellet was resuspended in disruption buffer (100 mM Tris-HCl [pH 8.1], 100 mM KCl, 5 mM $MgCl_2$, 5% [wt/vol] glycerol, 50 mM octylglucoside, 10 mg of lysolecithin per ml, 1.5 mM dithiothreitol) and incubated at 31°C for 25 min. vRNPs were purified by centrifugation at 45,000 rpm for 4 h at 4°C in an SW 50.1 rotor through a step gradient (1 ml of 70%, 0.75 ml of 50%, 0.375 ml of 40%, and 1.8 ml of 33% [wt/vol] glycerol), with gradient components diluted in 50 mM Tris (pH 7.8)–150 mM NaCl. Fractions (385 μl) were harvested manually from the gradient and, a 10-μl aliquot of each was analyzed on a sodium dodecyl sulfate-polyacrylamide gel electrophoresis (SDS-PAGE) minigel to check the presence of the viral proteins. vRNPs devoid of detectable M1, HA, and NA proteins, as judged by Coomassie blue staining, were present in fractions 7 to 11. The vRNP peak fractions were pooled, diluted with 4 volumes of microinjection buffer (10 mM Tris, 120 mM KCl [pH 7.4]), and centrifuged at 35,000 rpm for 2 h at 4°C in an SW 50.1 rotor. The vRNP pellet was resuspended in 50 μl of microinjection buffer (to a concentration of approximately 0.5 μg/μl), aliquoted, and stored at −70°C.

For microinjection, cells were seeded 2 days prior to use onto scored-glass coverslips (Bellco Biotechnology) coated with poly-L-lysine. Microinjection was done on a Zeiss inverted microscope with a 5242 Eppendorf microinjector. Before injection, cells were transferred to MEM containing 20% FCS and 20 mM HEPES (pH 7.3). The cells were injected at room temperature and then incubated for 90 min at 37°C under 5% CO_2 in growth medium containing 1 mM cycloheximide before they were fixed and analyzed by immunofluorescence microscopy. We estimated that the volume of material injected was approximately 1/10 of the cell volume.

Cytosol acidification. A mild acidification of the cytosol of CHO cells was achieved by the "NH_4Cl prepulse" protocol as essentially described by Sandvig et al. (40). This approach was chosen because it was best tolerated by cells, and the cells remained viable and functional. Monolayer cells were preloaded with 40 mM NH_4Cl in growth medium for 15 min at 37°C. NH_4Cl diffuses quickly throughout the cell. The prepulse medium was then replaced by postpulse medium lacking NH_4Cl (140 mM KCl, 2 mM $CaCl_2$, 1 mM $MgCl_2$, 20 mM HEPES [pH 7.0], 1 mM amiloride) for 15 min at 37°C. Upon removal of the extracellular NH_4Cl, the NH_3 rapidly diffused from the cell, leaving behind an excess of H^+ ions; i.e., the cytosol was temporarily acidified. To sustain the acidification, extracellular NaCl was replaced by KCl and the Na^+/H^+ exchanger was inhibited by amiloride (1).

To qualitatively assess that there was indeed a significant drop in intracellular pH resulting from the above method, the pH was monitored by using a pH-sensitive fluorochrome, 2′,7′-bis-(2-carboxyethyl)-5-(and-6-)-carboxyfluorescein acetoxymethyl ester (BCECF-AM) (Molecular Probes). BCECF-AM readily diffuses across cellular membranes and is efficiently retained when the ester moiety is hydrolyzed by cellular esterases (38). Cells grown on narrow rectangular glass coverslips were incubated for 15 min at 37°C with 1 mM BCECF-AM in regular growth medium prior to acidification. The emitted fluorescence was determined by inserting the coverslips into a cuvette containing postpulse medium and quantifying fluorescence emissions with a Hitachi F-2000 fluorescence spectrophotometer at two wavelengths, 492 and 520 nm. The ratio of the two wavelengths controls for differential loading of the BCECF-AM into cells, since the 492-nm emission wavelength is insensitive to pH. To calibrate the BCECF-AM fluorescence with set pH values, cells were placed in prepulse medium at pH 5.5, 6.0, 6.5, 7.0, and 7.5 containing 1 mM nigericin, a proton ionophore that equilibrates extracellular and intracellular pH gradients (see Fig. 5A) (40). Qualitatively, the extent of acidification was seen to be below pH 6.0, below which the sensitivity of BCECF-AM is attenuated.

Gradient centrifugation and immunoprecipitation. Cells were grown for 1 day on 60-mm dishes to a density of 2×10^6 cells per ml. After the experiment, cells were swollen in low-salt buffer (10 mM NaCl, 0.25 mM MES, 0.25 mM Tris [pH 7.5]), scraped, and homogenized mechanically with 26 strokes through a 25-gauge needle. The extent of homogenization was nearly 90% cell breakage as determined by trypan blue exclusion. The homogenate was centrifuged for 10 min at 5,000 × *g* at 4°C. The low-speed supernatant was loaded onto a discontinuous glycerol gradient with identical composition to the gradients used to isolate vRNPs for microinjection (see above). The gradients were centrifuged at 45,000 rpm for 4 h at 4°C in an SW 50.1 rotor.

Fractions (384 μl) were collected from the top of the gradient and immunoprecipitated with 10 μl of anti-M1 or anti-NP polyclonal antiserum and 100 μl of 10% protein A-Sepharose–MNT–0.5% Triton X-100. The immune complexes were incubated for 16 h at 4°C, washed twice with 0.5% Triton X-100–MNT, and analyzed by SDS-PAGE followed by autoradiography.

Cell fusion assay. 3PNP-4 cells were grown for 2 days on round 12-mm glass coverslips treated with poly-L-lysine. The cells were transferred to serum-free medium 16 h before fusion. HeLa cells (10^5) were seeded onto the same coverslips and allowed to attach at 37°C for 2 h. Cells were fused with polyethylene glycol (PEG) (5). Coverslips were washed with calcium- and magnesium-free PBS containing 1 g of glucose per liter and then inverted onto a drop of 50% PEG 8000 (Sigma) made up in PBS-glucose. The PEG solution was prepared by autoclaving 10 g of solid PEG, which was then mixed with 10 ml of PBS-glucose. After 2 min at room temperature, the coverslip was washed three times with PBS-glucose and returned to MEM containing 1 mM cycloheximide (to prevent further protein synthesis) for 60 min before fixation. The coverslips were subsequently processed for immunofluorescence microscopy.

For cell fusion assays, L929 cells and HeLa cells were chosen because their nuclei could be easily distinguished from each other. L929 cells were seeded onto round 12-mm no. 1 coverslips coated with poly-L-lysine and incubated for 2 days to a density of approximately 2×10^5 cells per coverslip. The cells were infected with virus at a MOI of 1 to 2 PFU per cell in RPMI 1640 medium containing 0.2% BSA and buffered to pH 6.8 with 20 mM HEPES. The cells were then incubated at 37°C for 6 h. HeLa cells (10^5) were then seeded onto the same

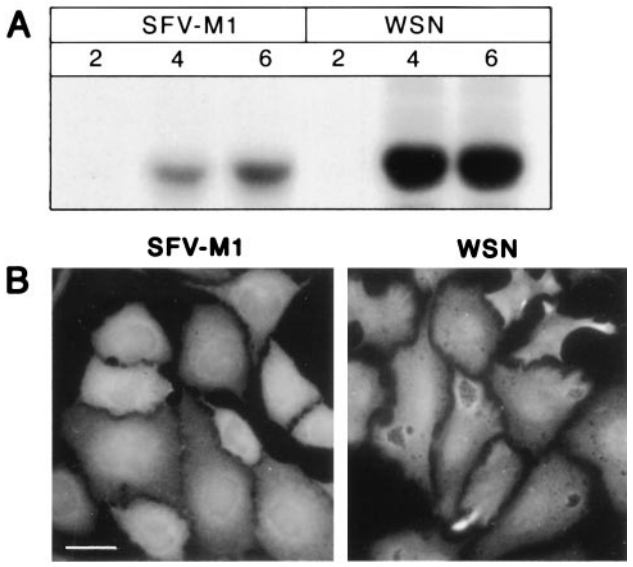

FIG. 1. Expression of M1 by a recombinant SFV (SFV-M1) at various times after infection. (A) CHO cells infected with SFV-M1 at 5 PFU per cell were radioactively labeled with [^{35}S]methionine-[^{35}S]cysteine for 30 min at 2, 4, or 6 h postinfection, immunoprecipitated with anti-M1 antibodies, and analyzed by SDS-PAGE (12% polyacrylamide) followed by autoradiography. (B) CHO cells infected with either SFV-M1 or WSN and analyzed by immunofluorescence microscopy at 5 h postinfection with anti-M1 antibodies. Bar, 25 μm.

coverslip at 4 h postinfection and allowed to attach to the coverslip for 2 h at 37°C in MEM containing 2% FCS. After cell fusion, the heterokaryon was acidified by the NH_4Cl prepulse method and then incubated in complete medium with 1 mM cycloheximide for 60 min before fixation and processing for immunofluorescence microscopy.

To visualize nuclei, cells were incubated with 1 μg of bis-benzimide (Hoechst no. 33258; Sigma) per ml for 1 min. This dye gave differential staining of mouse cell nuclei and human cell nuclei, allowing an easy distinction to be made between the infected and uninfected nuclei. L929 and 3PNP-4 cell nuclei were relatively small and stained brightly, with many very bright speckles. HeLa cell nuclei, however, tended to be larger, stained less brightly overall, with some dark areas.

RESULTS

Expression of recombinant M1 by SFV-M1. As an initial approach to study the effects of M1 on vRNP nuclear transport, we established an expression system for M1 by using the SFV vector. When CHO cells were infected with SFV-M1 and radioactively labeled with [^{35}S]methionine-[^{35}S]cysteine for 30 min at 2, 4, or 6 h postinfection, immunoprecipitation of cell lysates with anti-M1 antibodies showed that M1 expression was detectable between 2 and 4 h after infection (Fig. 1A). By 8 h, the amount of M1 was approximately 60% of that synthesized during an 8-h influenza virus infection as determined by Western blotting (immunoblotting) (data not shown). While the level of M1 expression was lower than that observed during normal influenza virus infection (WSN strain), it was considerably higher than obtained with other expression systems. A further advantage was that every cell expressed M1 (Fig. 1B). The intracellular localization of M1, assayed at 5 h postinfection by indirect immunofluorescence microscopy showed a uniform staining throughout the cytoplasm and nucleus (Fig. 1B). However, M1 synthesized during normal influenza virus infection showed a higher signal within the nucleus compared with the recombinant M1. Similar staining patterns were obtained for MDBK cells. However, CHO cells were more suitable for morphology analysis by immunofluorescence microscopy.

Nuclear import of vRNPs is inhibited by M1. To test whether M1 binding prevents the import of vRNPs from the cytosol to the nucleus, the fate of vRNPs entering cells that expressed recombinant M1 was determined. It was of interest to know whether the newly synthesized, recombinant M1, in contrast to the M1 of the incoming virus, would bind to the vRNPs and prevent their entry into the nucleus. The M1 gene from WSN influenza virus was expressed by using the recombinant SFV expression system (22). A mutant SFV, called SFV-M1, was produced which expressed M1 and the nonstructural proteins of SFV but none of the structural proteins of SFV (see Fig. 1).

The effect of the expressed M1 on incoming influenza virus was next determined by immunofluorescence microscopy with monoclonal antibodies to NP. Here and in subsequent experiments, we monitored the location of the vRNPs by staining for NP. CHO cells were first infected with wild-type SFV or control recombinant SFV expressing foreign proteins at 5 PFU per cell and 5 h later with a high MOI of influenza virus at 150 to 200 PFU per cell. To ensure that we were detecting only the NPs of the incoming viruses, the infection was carried out in the presence of cycloheximide. This protein synthesis inhibitor does not affect vRNP import into the nucleus (26) but prevents the generation of new viral proteins.

When cells were infected with SFV-M1 prior to influenza virus infection, the incoming vRNPs did not reach the nucleus (Fig. 2g and h). They remained localized in the cytoplasm, displaying a scattered punctate staining pattern similar to that previously observed for viruses entering cells in the presence of amantadine, which prevents nucleocapsid dissociation and vRNP import into the nucleus (2, 25).

Several controls were performed to determine whether the effect observed was due to expression of M1. When cells were not infected with SFV, the incoming vRNPs were transported efficiently into the nucleus as shown by a distinct nuclear staining with anti-NP antibodies (Fig. 2a). The incoming M1 gave a weak and diffuse staining throughout the cytosol and the nucleus (Fig. 2b). When influenza virus entered cells preinfected with wild-type SFV, bright staining with antibodies against the spike glycoproteins E1 and E2 of SFV could be observed (Fig. 2d) and the incoming vRNPs were again efficiently imported into the nucleus (Fig. 2c). In a third control, cells were infected with a recombinant SFV, SFV-lacZ, expressing β-galactosidase. In these cells, vRNP import into the nucleus was also uninhibited (Fig. 2e and f).

Taken together, these controls indicated that SFV infection, per se, and the expression of a foreign protein did not affect the normal entry of influenza virus into the nucleus. Thus, the results clearly indicated that it was the presence of newly synthesized M1 that blocked vRNP import into the nucleus. A substantial amount of M1 was apparently needed to achieve this block, since a stable CHO cell line, which constitutively expressed low levels of M1 (approximately 5% of an influenza virus infection), was unable to prevent vRNP import (results not shown).

Microinjected vRNPs are inhibited from nuclear import by M1 expression. To determine whether the M1-induced block occurred at the level of the cytosol and to rule out any defects in virus binding and internalization, purified vRNPs were microinjected into the cytoplasm of M1-expressing cells. This approach circumvented the endocytosis and membrane fusion steps in the entry process. In agreement with earlier studies (16), the vRNPs microinjected into control cells not expressing M1 were imported into the nucleus (Fig. 3a and b). The same was observed when cells were infected with wild-type SFV (Fig. 3c and d) or SFV-lacZ (data not shown).

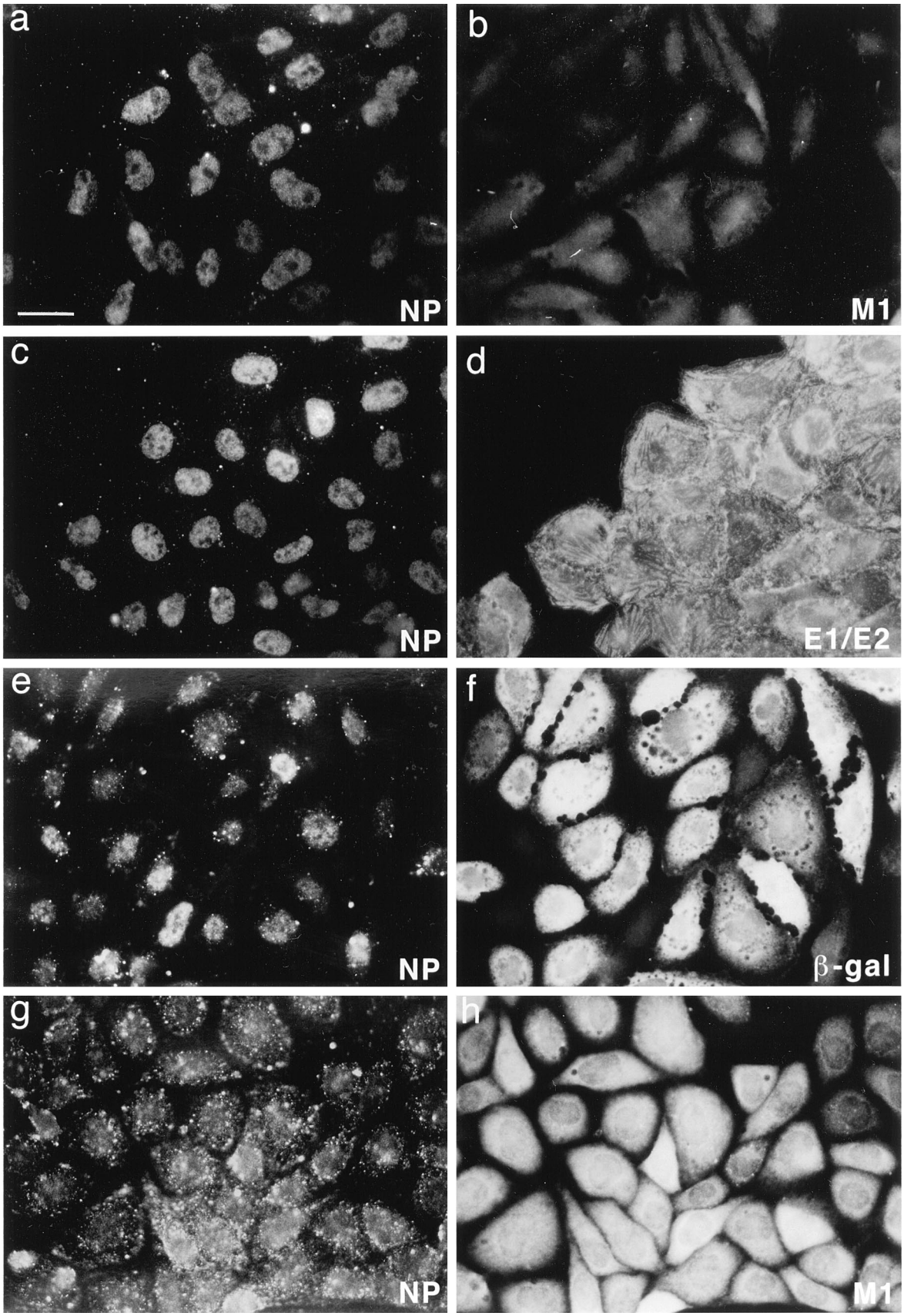

FIG. 2. Expression of M1 by SFV-M1 inhibits the nuclear import of incoming vRNPs. The fate of incoming vRNPs was analyzed by immunofluorescence microscopy with an anti-NP antibody (a, c, e, and g). CHO cells were mock infected with SFV (a and b) or initially infected for 5 h at 5 PFU per cell with either wild-type SFV (c and d), SFV-lacZ expressing β-galactosidase (e and f), or SFV-M1 expressing M1 (g and h). A high MOI of influenza virus at 150 to 200 PFU per cell was used to superinfect cells in order to detect incoming vRNPs. Cycloheximide (1 mM) was added during the influenza virus infection to prevent the synthesis of new viral proteins. The expression of proteins by wild-type SFV, SFV-lacZ, and SFV-M1 were detected with antibodies against the E1/E2 glycoproteins (d), β-galactosidase (β-gal) (f), and M1 (b and h), respectively. Bar, 25 μm.

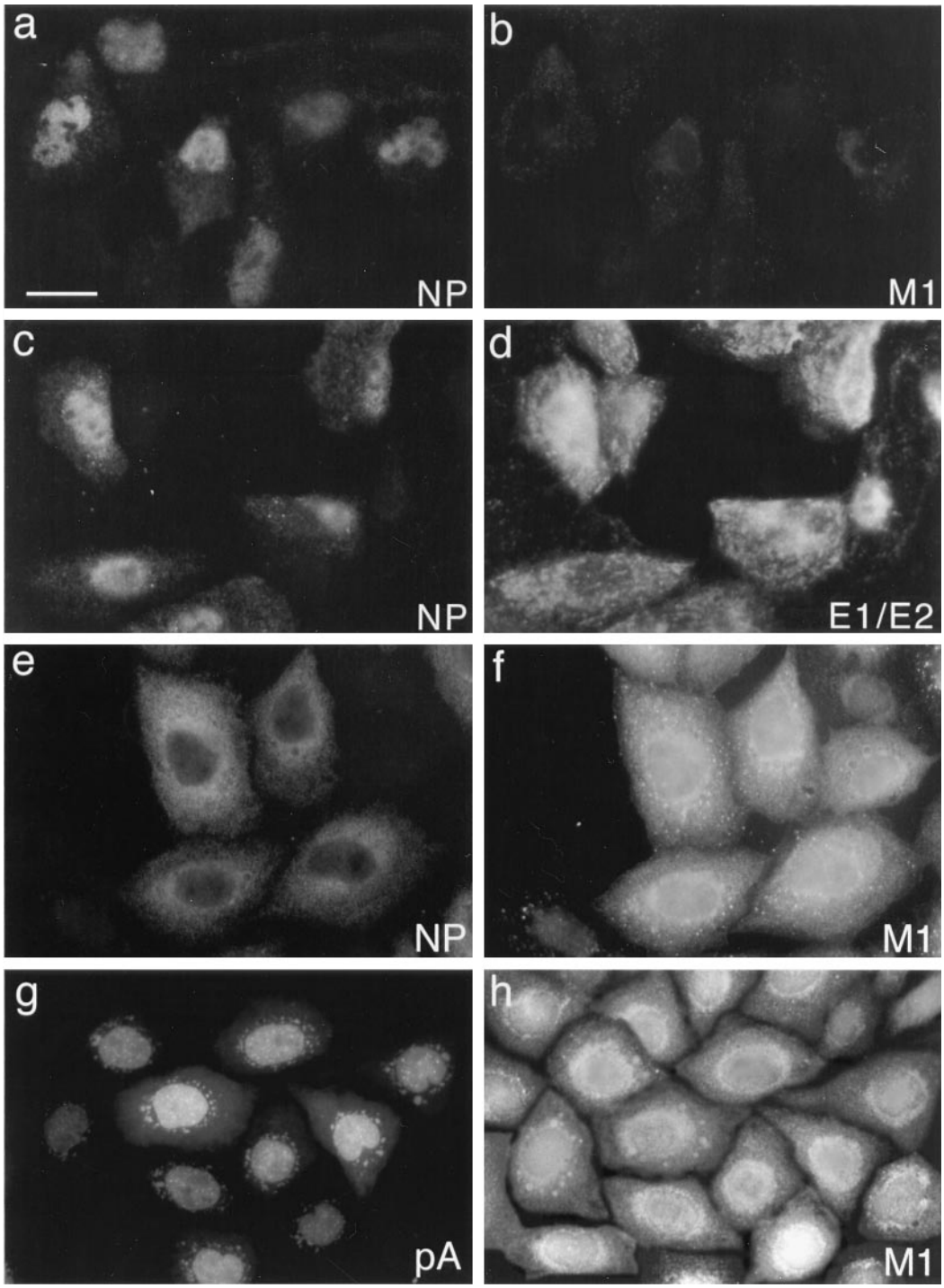

FIG. 3. Expression of M1 prevents the nuclear import of microinjected vRNPs. vRNPs were prepared from detergent-treated virus, fractionated on glycerol gradients, and purified for microinjection. The localization of vRNPs was analyzed by immunofluorescence microscopy with anti-NP antibodies (a, c, e, and g) at 90 min after microinjection into CHO cells mock infected with SFV (a and b) or cells that were previously infected for 5 h at 5 PFU per cell with wild-type SFV (c and d) or SFV-M1 (e and f). The expression of proteins by wild-type SFV and SFV-M1 was detected with antibodies against the E1/E2 glycoproteins (d) and M1 (b, f, and h), respectively. To be sure that M1 expression did not impair generalized nuclear uptake, fluorescein isothiocyanate-protein A, a highly karyophilic molecule, was microinjected into M1-expressing cells. Bar, 25 μm.

In contrast, when cells expressing M1 from the recombinant SFV-M1 were microinjected, the vRNPs did not enter the nucleus (Fig. 3e) but remained in the cytoplasm and displayed a diffuse staining pattern. To rule out a general defect in nuclear import as a result of M1 expression, a karyophilic protein, fluorescein isothiocyanate-protein A, was microinjected. Protein A enters nuclei via nuclear pore complexes by using an active uptake mechanism (21). It was efficiently imported into the nucleus of M1-expressing cells (Fig. 3g and h). This indicated that the presence of newly synthesized M1 in the

cytosol specifically prevented the import of vRNPs from the cytosol into the nucleoplasm.

Acidification of cytosol reverses the import block. To test the idea that exposure to low pH results in the dissociation of M1 from vRNPs, experiments were performed in which the cytosol of M1-expressing cells was acidified during influenza virus entry. If M1 is, indeed, sensitive to low pH, its association with the incoming vRNPs should be lost after such treatment, and the incoming vRNPs should be able to reach the nucleus. Previous in vitro experiments with isolated virus by Zhirnov (57, 58) have shown the dissociation of M1 from vRNPs at acidic pH. However, it is not known if this acid-dependent M1 dissociation was actually happening within the infected cell.

Transient acidification of the cytosol to pH values approaching that of the late endosome (pH 5.0 to 5.5) can be achieved by the NH_4Cl-prepulse protocol (see Materials and Methods) (40). This procedure caused a rapid and transient intracellular pH drop to values below 6.0 for a period of 1 min and then an increase to about pH 6.5 within 3 min (Fig. 4A). The extent of acidification observed was in agreement with previous studies (9, 31, 40).

Surface-bound influenza virus was internalized for 30 min to allow the vRNPs of the incoming virus to penetrate into the cytosol. The $t_{1/2}$ of vRNP penetration into the cytosol had previously been determined to be 25 min (26). The cytosol was then acidified by the NH_4Cl-prepulse protocol. The incoming vRNPs were observed by immunofluorescence microscopy to be imported normally into the nucleus (Fig. 4B, panels a and b). This showed that the transient acidification, per se, had no deleterious effects on nuclear transport. However, the small amount of punctate cytoplasmic NP staining could represent viruses that were trapped in the early stages of endocytosis, since cytosol acidification has been shown to inhibit endocytosis by coated pits (40).

When incoming vRNPs were internalized into M1-expressing cells and the cytosol was acidified, the normal block in import was reversed. Rapid import of vRNPs into the nucleus was observed (Fig. 4B, panels e and f). The import was acidification dependent, because vRNP import was inhibited in M1-expressing cells which were not acidified (Fig. 4B, panels c and d). The result indicated that the capacity of M1 to interfere with vRNP import was lost by brief acidification of the cytosol. This strongly supported the hypothesis that exposure to mildly acidic pH affects the properties of M1.

M1 binds to incoming vRNPs and is dissociated with cytosol acidification. The most likely explanation for the block in the nuclear import of vRNPs was a direct association of M1 with incoming vRNPs. To investigate biochemically whether such an association occurred, we analyzed the sedimentation of M1 during ultracentrifugation in discontinuous glycerol gradients. Lysates were prepared from control M1-expressing cells or M1-expressing cells exposed to incoming influenza virus.

The gradient system used was based on a protocol for isolating vRNPs from purified virus (16), a procedure that we routinely used to prepare vRNPs for microinjection. To demonstrate the mobility of incoming vRNPs from infected cells on such gradients, CHO cells were infected with [^{35}S]methionine-[^{35}S]cysteine-radiolabeled virus and allowed to internalize the virus for 90 min in the presence of cycloheximide. The cells were homogenized mechanically without detergents, and the cell lysate was clarified of insoluble materials by low-speed centrifugation. This supernatant was then applied to the glycerol gradients for ultracentrifugation. Following immunoprecipitation with anti-NP antibodies and as indicated by the position of the NP band after SDS-PAGE and autoradiography, the vRNPs from ^{35}S-radiolabeled viruses sediment as a broad

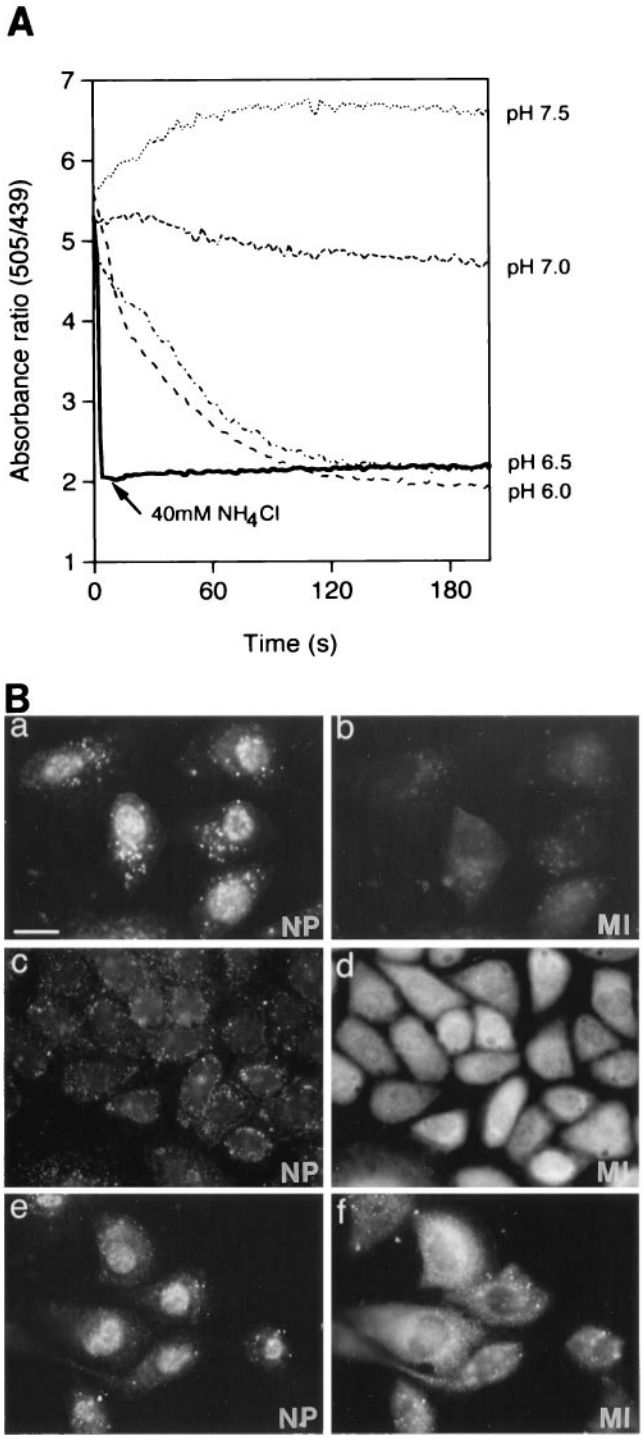

FIG. 4. Cytosol acidification reverses the M1 block on vRNP nuclear transport. (A) To qualitatively show that a drop in intracellular pH was observed by the NH_4Cl prepulse technique used to acidify the cytosol of CHO cells, cells were loaded with a pH-sensitive fluorescent probe, BCECF-AM, and changes in emitted fluorescence was measured with a spectrophotometer. The range in emitted fluorescence was calibrated in cells treated with nigericin, an ionophore that equilibrates intracellular and extracellular pH, and solutions with known pH values. (B) The effect of cytosol acidification on influenza virus infection was analyzed by immunofluorescence microscopy with anti-NP antibodies (a, c, and e) and anti-M1 antibodies (b, d, and f). A high MOI of influenza virus (200 PFU per cell) was internalized for 30 min at 37°C, and cell cytosol was acidified and analyzed after a 60-min incubation (a and b). Cells were previously infected with SFV-M1 for 5 h before internalization of a high MOI of influenza virus without cytosol acidification (c and d). In a parallel situation, the cytosol of these cells was acidified (e and f). Bar, 25 μm.

peak in fractions 6 to 11 (Fig. 5A). An identical distribution of NP was found when detergent-solubilized purified virus was analyzed on similar gradients as determined by Coomassie blue staining (data not shown).

To analyze the sedimentation behavior of intracellular M1 in the absence of other influenza proteins, CHO cells were infected with 5 PFU of SFV-M1 per cell and subsequently labeled with [^{35}S]methionine-[^{35}S]cysteine between 3 and 5 h postinfection to radiolabel the synthesized M1 protein. A detergent-free, low-speed supernatant was applied to the glycerol gradients for ultracentrifugation. Following centrifugation, the fractions were precipitated with anti-M1 antibodies and analyzed by SDS-PAGE. As shown in Fig. 5B, all of the soluble M1 protein was recovered in the top four fractions of the gradient. The M1 population in these fractions is believed to be in its free form, since M1 which is extracted by high salt and detergents from purified virions also migrates in at the same fractions on identical gradients (data not shown).

An altered gradient distribution of M1 was found when the same experiment was repeated for M1-expressing CHO cells in which a high MOI of nonradiolabeled influenza virus (150 to 200 PFU per cell) was allowed to internalize for 90 min immediately following the 2-h M1 radiolabeling period. Cycloheximide was added to prevent any further protein synthesis, such that M1 was the only viral protein which was radiolabeled. While the majority of M1 still remained at the top of the gradient, approximately 30% of the soluble M1 sedimented in the part of the gradient containing the incoming vRNPs within fractions 7 to 11 (Fig. 5A and C). This shift in M1 mobility was apparently due to association with incoming vRNPs.

That the recombinant M1-vRNP complexes observed in the gradient were actually formed between M1 and cytosolic vRNPs rather than with vacuolar viruses was shown by using an ammonium chloride (NH_4Cl) control. This acidotropic drug elevates the pH in endosomes (31) and prevents the penetration of influenza virus nucleocapsids into the cytosol by membrane fusion (28). The inclusion of NH_4Cl prevented the exposure of incoming vRNPs to the cytosol and their association with cellular recombinant M1. In Fig. 5D, M1 remained at the top of the gradient and did not show a shift in sedimentation mobility. Thus, for M1-vRNP complexes to form, penetration of vRNPs into the cytosol was required. Taken together, the results showed that vRNPs formed complexes with the newly synthesized M1 in the cytosol and resulted in a detectable gradient shift. As incoming vRNPs entered the cytosol, the M1 that was present in the virus particle presumably dissociated according to the normal uncoating program but was immediately replaced by some of the newly synthesized recombinant M1. This was the likely reason why the vRNPs failed to enter the nucleus.

To test whether low pH could disrupt the interaction between recombinant M1 and incoming vRNPs, the cytosol of M1-expressing cells was acidified by the NH_4Cl prepulse protocol and the distribution of M1 was analyzed by the gradient centrifugation assay. Figure 5E demonstrated that cytosolic acidification caused the vRNP-associated M1 in fractions 6 to 11 to dissociate and therefore to shift in mobility to the top four fractions of the gradient.

Native M1 dissociates from newly synthesized vRNPs with cytosol acidification. We next used the gradient centrifugation assay described above to analyze the effect of acidic pH on the interaction between newly synthesized vRNPs and native M1 at late times of infection. Influenza virus-infected CHO cells were radiolabeled with [^{35}S]methionine-[^{35}S]cysteine during a 2-h period starting 5 h postinfection. At this time, most of the newly assembled vRNPs have been transported from the nucleus to the cytosol, where they remained associated with M1 (25). The cytosol of these cells was acidified by using the NH_4Cl prepulse protocol. The cells were then solubilized with Triton-X100, the low-speed supernatant was subjected to sedimentation on glycerol gradients, and the fractions were analyzed by immunoprecipitation with antibodies to the whole virus.

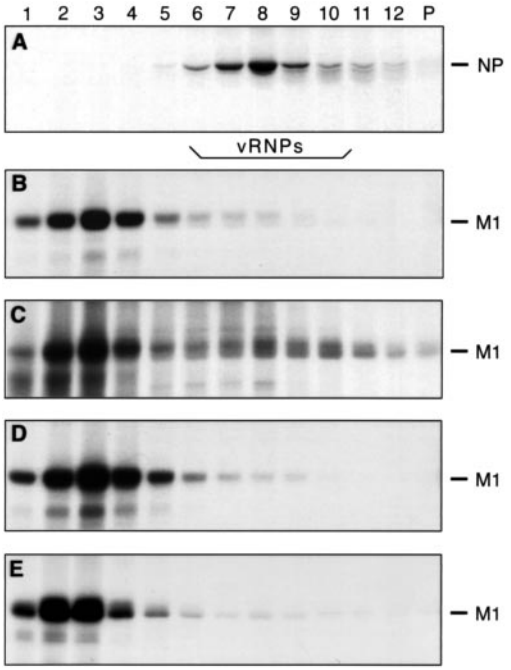

FIG. 5. Recombinant M1 binds to incoming vRNPs. The association of heterologous M1 and incoming vRNPs was analyzed by ultracentrifugation in glycerol gradients. (A) The mobility of incoming vRNPs was determined by infecting CHO cells with [^{35}S]methionine-[^{35}S]cysteine-labeled WSN virus. The cells were homogenized, and a low-speed supernatant was applied to the gradient. Fractions were collected, immunoprecipitated with anti-NP antibodies, and analyzed by SDS-PAGE followed by autoradiography. (B) CHO cells were infected with 5 PFU of SFV-M1 per cell and labeled with [^{35}S]methionine-[^{35}S]cysteine between 2 and 5 h postinfection. The cells were homogenized, and a low-speed supernatant was applied to a glycerol gradient. Collected fractions were immunoprecipitated with anti-M1 antibodies. (C) In addition, influenza virus (WSN) at a high MOI (150 to 200 PFU per cell) was internalized for 60 min at 37°C in cells expressing radiolabeled M1 in the presence of 1 mM cycloheximide followed by gradient centrifugation, fractionation, and immunoprecipitation as before. (D) As a negative control to show that the M1 shift was due to an association with vRNPs in the cytosol, influenza virus was internalized in the presence of 30 mM NH_4Cl, which blocks viral penetration into the cytoplasm. (E) To demonstrate that M1 dissociated from the vRNPs by exposure to low pH, the cytosol of cells containing M1-vRNP complexes was acidified by the NH_4Cl prepulse protocol after 60 min of high-MOI (150 to 200 PFU per cell) influenza virus internalization.

In control cells that had not been acidified, M1 migrated in all fractions from 1 to 11 (Fig. 6A). Fractions 6 to 11 contained the vRNPs as indicated by the comigration of NP and polymerase. However, when the cytosol of the cells had been acidified prior to cell lysis, M1 sedimented almost exclusively in the top five fractions of the gradient, where free M1 normally migrates (Fig. 6B). A similar result was obtained when the cytosol from cells that had not been acidified prior to lysis was acidified in vitro with added pH 5.0 MES-buffered lysis solution prior to gradient centrifugation (Fig. 6C). The NP and polymerase profiles were unaffected by the two methods used to acidify the cytosol (data not shown). Thus, the M1 mobility shift from the middle to the top of the gradient was due to its acid-induced dissociation from vRNPs. These results indicated

that the association of M1 with vRNPs could be reversed by exposure to low pH. Dissociation could be induced by acidification in live cells and also in a cell lysate. Taken together, the results provided the first direct evidence that acidification does, indeed, affect the capacity of M1 to bind to vRNPs in the cytosol and to prevent their uptake into the nucleus in live cells.

Acidification of the cytosol allows reimport of newly synthesized vRNPs into the nucleus. In a previous study, a temperature-sensitive M1 mutant from *ts*51 virus was used to show that the functions of M1 include the prevention of nuclear reimport of vRNPs newly exported from the nucleus into the cytosol (53). Having shown that M1 could be dissociated from such cytosolic vRNPs by acidification of the cytosol of the infected cell, it was of interest to determine whether the vRNPs were now free to reenter the nucleus.

To assess nuclear import, it was necessary to have nuclei present that did not already contain some NP. To achieve this, a cell fusion approach was used to analyze heterokaryons produced by fusing infected and uninfected cells. Briefly, infected L929 cells at late times of infection were fused with uninfected HeLa cells and the uptake of vRNPs into the HeLa cell nuclei was assayed by immunofluorescence microscopy (Fig. 7b and e). Conveniently, the HeLa cell nuclei (small arrows) and L929 cell nuclei (large arrows) can be easily distinguished by their Hoechst staining patterns (53).

First, we confirmed the observation made previously (53) that newly synthesized vRNPs exported from the infected L929 cell nuclei into the cytosol failed to enter the uninfected HeLa cell nuclei (Fig. 7b). The NP staining was distributed throughout the heterokaryon, with notable exclusion from the nuclei. The M1 staining was predominantly cytosolic (Fig. 7c).

In contrast, if the heterokaryon cytosol was acidified by the NH_4Cl washout protocol, the exported vRNPs were capable of import into the uninfected nuclei (Fig. 7e, small arrows). The M1 distribution was unaltered; i.e., a uniform staining throughout the heterokaryon was seen (Fig. 7f). Interestingly, although the acidified vRNPs could be imported into the uninfected nuclei, they failed to be reimported into the infected L929 cell nuclei (Fig. 7e, large arrows). It remained unclear why these previously infected nuclei were unable to support reimport (53).

Overall, these results indicated that acidification of the cytosol relieves not only the M1-induced nuclear import block for incoming vRNPs but also the block in reimport of newly assembled vRNPs into an uninfected nucleus.

M1 has no effect on nuclear import of free NP. Finally, it was important to determine whether M1 had any effect on the nuclear transport of free NP, the most abundant structural protein of the vRNP complex, since recent reports have implicated NP in targeting the vRNP into the nucleus (31). We used the 3PNP-4 cell line which constitutively expresses NP (20) and asked whether M1 expression would prevent the nuclear targeting of NP. Again, using the heterokaryon assay, 3PNP-4 cells showed NP accumulation within the nucleus with no M1 signal prior to cell fusion, (Fig. 8b and c, small arrows). Conversely, HeLa cells infected with SFV-M1 showed significant M1 staining with no NP signal (Fig. 8b and c, large arrows). HeLa cells expressing M1 were fused at 5 h postinfection with 3PNP-4 cells, and the distribution of NP was determined by immunofluorescence microscopy in the absence of cycloheximide. The data showed that NP was efficiently imported into the HeLa cell nucleus within the 60 min after fusion (Fig. 8h), although M1 was distributed throughout the heterokaryon (Fig. 8g). Within the heterokaryon, the 3PNP-4 nuclei show a brighter signal due to NP accumulation prior to cell fusion.

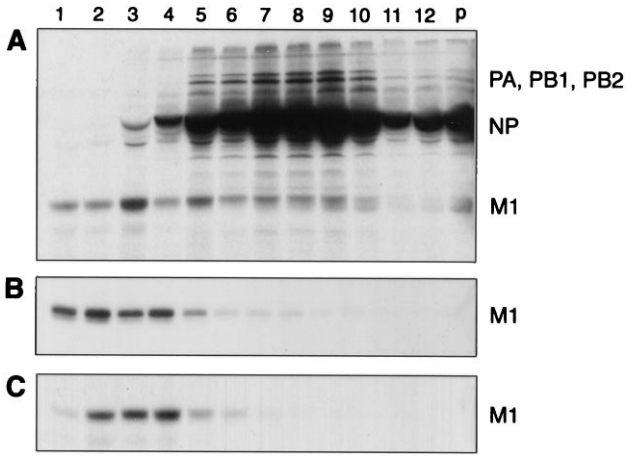

FIG. 6. Cytosol acidification causes the release of M1 from vRNPs. The association of M1 with newly synthesized vRNPs was analyzed by gradient centrifugation. CHO cells were infected with 5 PFU of WSN per cell and metabolically labeled with [^{35}S]methionine-[^{35}S]cysteine during a 2-h period starting 5 h postinfection. A cell lysate was applied to glycerol gradients, fractionated, and immunoprecipitated with anti-WSN antibodies recognizing viral structural proteins. The distribution of M1 is shown without cytosol acidification (A), after acidification by the NH_4Cl washout protocol (B), or after exposure to pH 5.0 at the time of lysis (C).

From the data, it could be concluded that M1 does not intervene in the nuclear import of free NP. Thus, M1 binding is likely to be specific for vRNP complexes.

DISCUSSION

An in situ approach was taken to analyze the interaction between M1 and vRNPs and the consequences of this interaction on nuclear transport of the vRNPs. When viruses were allowed to enter cells that expressed recombinant M1, the incoming vRNPs associated with the M1 present in the cytosol and transport to the nucleus was inhibited. Thus, while the M1 of the incoming virus particle was probably dissociating normally, it was replaced by cytosolic M1 molecules that had not been exposed to low pH. Brief acidification of the cytosol resulted in dissociation of the newly bound M1, and nuclear import of the vRNPs occurred. These findings provide experimental evidence for the long-standing hypothesis that low pH can prime influenza virus capsids for disassembly by specifically causing M1 dissociation and allowing the vRNPs to enter the nucleus (25).

It is well known that influenza virus penetration into the cytosol is triggered by an acid-activated, HA-mediated membrane fusion reaction in late endosomes. That vRNP import after the fusion event might also depend on exposure to low pH has been entertained as a possibility for some time (25, 27). Originally, the hypothesis was based on the mode of action of amantadine and the related rimantadine. These antiviral drugs affect M2, a membrane protein present in the viral envelope and in membranes of the infected cell (11, 19, 35, 46). Studies by Sugrue et al. indicated that M2 is an amantadine-sensitive proton channel and that it serves to neutralize the pH in the Golgi complex so that newly synthesized HA can be transported to the surface unmodified by low pH (46). It was subsequently shown that M2 is, indeed, an acid-activated, amantadine-sensitive channel for monovalent cations including protons (35, 41, 43, 49, 50).

The main antiviral effect of amantadine is manifested during influenza virus entry, not during late stages of infection (10, 15,

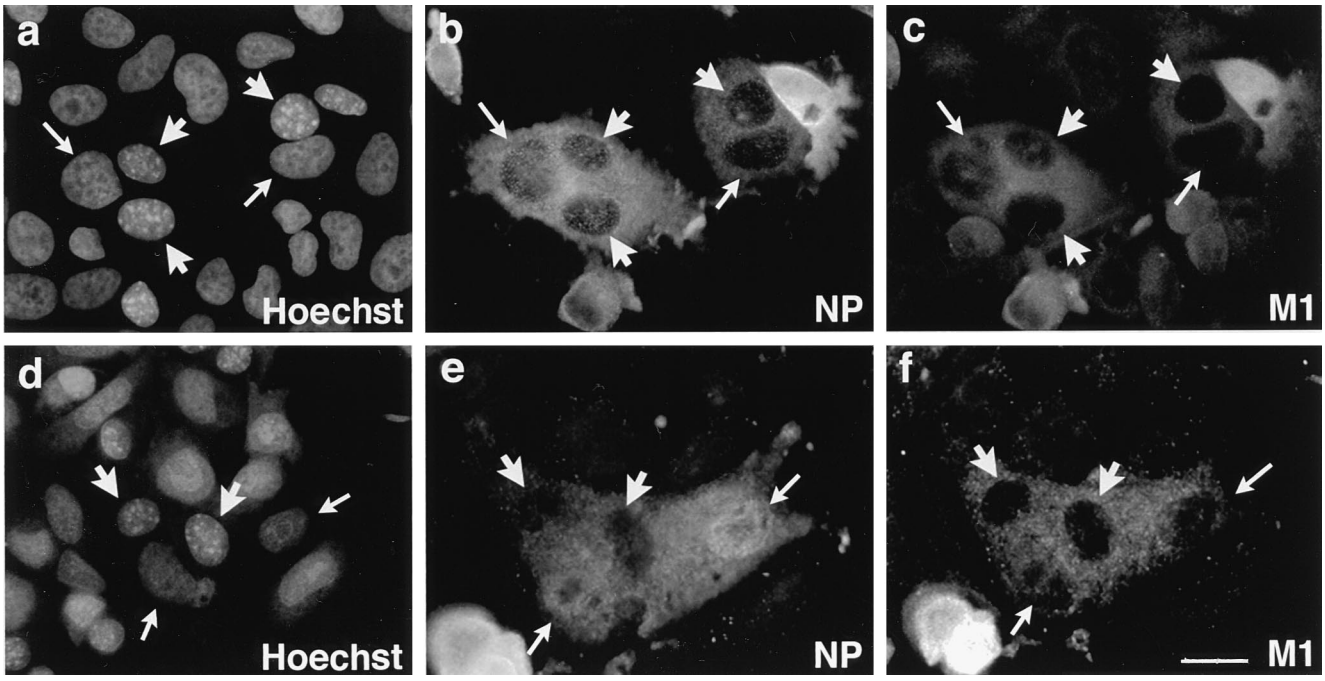

FIG. 7. Acidification of newly synthesized vRNPs allows reimport into the nucleus. A cell fusion approach was used to study the trafficking of vRNPs with and without cytosol acidification. L929 cells (large arrows) were infected with 5 PFU of WSN per cell and were fused with uninfected HeLa cells (small arrows) at 6 h postinfection. Cells were analyzed by fluorescence microscopy with the DNA stain Hoechst 33258 (a and d), with anti-NP antibodies (b and e) or with anti-M1 antibodies (c and f). The heterokaryon cytosol was either unacidified (a to c) or acidified (d to f) by the NH_4Cl washout protocol. Bar, 25 μm.

17). Following an observation made by Bukrinskaya et al. (2), we could show that amantadine prevented the import of incoming vRNPs into the nucleus as well as the dissociation of M1 and vRNPs, establishing indirectly a functional connection between M2 and downstream uncoating and nuclear targeting events. We proposed that during virus entry, M2 served as a conduit for protons into the virus particle, where the low pH somehow modified the association between M1 and vRNPs, priming them for dissociation (25).

It has, however, been difficult to obtain direct evidence for a causal relationship between acid exposure and nucleocapsid uncoating within the infected cell. One cannot, for example, use agents that prevent endosomal acidification, because they also inhibit the acid activation of HA and the vRNPs do not reach the cytosol. Data from in vitro experiments are compelling, but are limited in interpretation, providing only indirect evidence for the involvement of low pH in the cellular events of viral uncoating. Although it has been reported that low pH induces M1 dissociation from vRNPs of purified viruses in vitro (57, 58), the same effect can be observed in a pH-independent manner by using high salt and a detergent mixture (β-octylglucoside and lysolecithin) (36, 39). It is evident, however, that the vRNP as such does not require prior exposure to low pH to be competent for nuclear import, since purified M1-free vRNPs are import competent and infectious when microinjected into cells (16). One interesting feature of our system is that the cells are only acidified transiently, after which the pH rises to near neutrality. There thus appears to be no reassociation of M1 with vRNPs over time, and so it is likely that the effect of low pH on M1 is irreversible.

Several possible mechanisms may exist to account for how recombinant M1 might interfere with vRNP entry into the nucleus. First, M1 might interact with either cellular or viral factors involved in vRNP nuclear import and mask their nuclear import signals. NP and the polymerase subunits are known to enter the nucleus after synthesis in the cytosol and to possess the appropriate localization signals (4). Although NP does not have a classical nuclear localization sequence, work by O'Neill et al. indicates that it binds a cellular nuclear import factor, NPI-1, which is homologous to the alpha subunit of karyopherin. Furthermore, NP was shown to mediate the transport of heterologous RNA into the nucleus by using the "classical" nuclear transport pathway (32, 33). Although our results fail to show a direct association between NP and M1, it is possible that M1 still interacts with NP in the context of a vRNP complex or that M1 masks interactions of NP and NPI-1. Second, M1 binding could result in the association of vRNPs into complexes too large to be imported through the nuclear pores. Here, M1 might behave as a molecular glue to associate vRNPs into a nucleocapsid complex similar to that which is packaged into a virus particle. Third, recombinant M1 binding to vRNPs may cause the complex to bind to cytosolic surfaces of membranes acting via the lipid and RNA binding domains of M1. It is possible that with amantadine treatment, the failure of incoming M1 to see an acidic pH environment will prevent the release of vRNPs from the cytosolic surface of endosomes. The immunofluorescence microscopy of the incoming vRNPs in cells expressing M1 shows the same punctate distribution as seen for vRNPs in amantadine-treated cells (25).

Previously, we showed that M1 was required to promote export of the vRNPs from the nucleus of infected cells (25). Once exported, the vRNPs did not shuttle between the nucleus and cytoplasm but, rather, remained in the cytosol (53). Our observations that M1 association with vRNPs inhibited their nuclear import suggested an additional role for M1 during virus assembly; it prevents reimport of vRNPs into the nucleus of the infected cell and thus commits them to an assembly

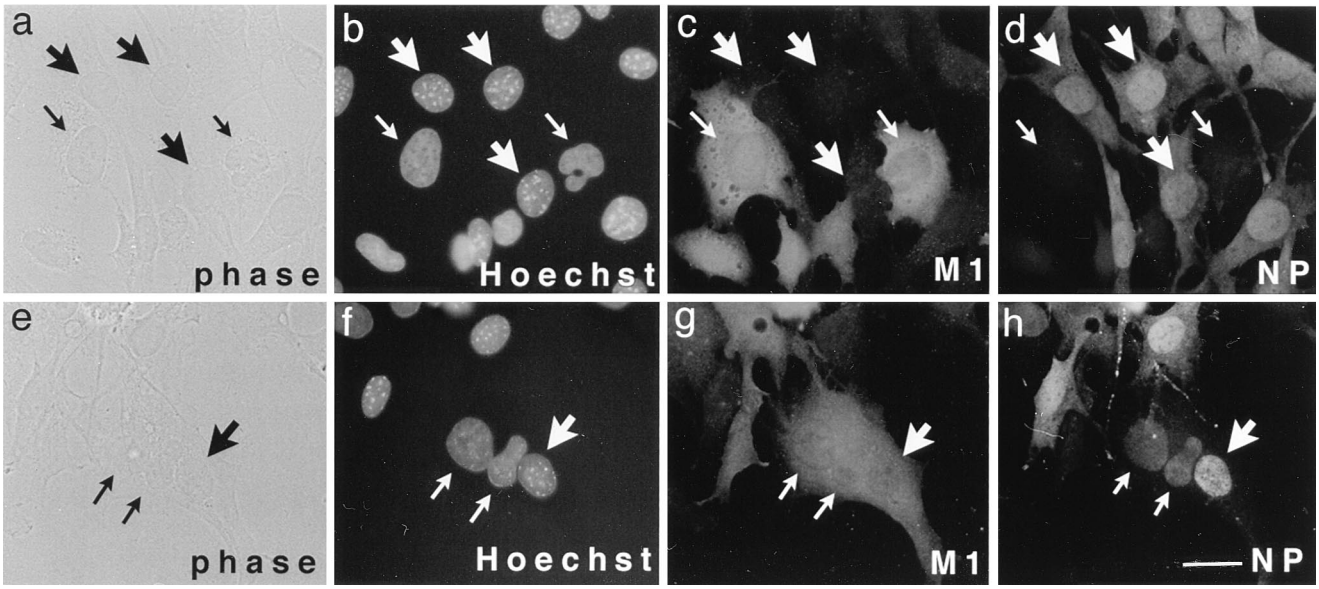

FIG. 8. M1 expression does not interfere with the nuclear transport of NP alone in the absence of viral RNA. 3PNP-4 cells (large arrows) were seeded alongside HeLa cells (small arrows) previously infected with SFV-M1 for 5 h. Cells were analyzed by phase-contrast microscopy (a and e), by fluorescence microscopy with the DNA stain Hoechst 33258 (b and f), with anti-M1 antibodies (c and g), or with anti-NP antibodies (d and h). Cells were either left unfused (a to d) or fused with PEG and analyzed after 60 min (e to h). Bar, 25 μm.

pathway leading to the budding of virus particles at the plasma membrane. If the infected-cell cytosol was subsequently acidified, M1 dissociated and the incoming vRNPs regained nuclear import competence. In the same manner, native M1 dissociated from newly synthesized vRNPs when exposed to low pH. Since we failed to observe nuclear reimport of vRNPs with cytosol acidification in infected cells during late times of infection, it was necessary to use a cell fusion approach to demonstrate that the vRNPs which had been exposed to low pH were import competent by providing an uninfected nucleus. As expected, the uninfected nuclei supported vRNP import whereas its infected counterpart nuclei failed to reimport. It was therefore likely that infected nuclei are no longer capable of accumulating vRNPs. Generalized nuclear import in these infected cells was not impaired since fluorescein isothiocyanate-protein A was imported efficiently into the nucleus following microinjection into the cytosol (53).

That a mechanism to prevent reimport is present in influenza virus-infected cells is interesting because not all viruses seem to have it. An example of a virus that seems to lack a reimport block is hepatitis B virus, a virus that replicates in the nucleus and buds from cytosolic membranes (for a review, see reference 14). Some of the replicated genomes are exported from the nucleus and assembled into capsids in the cytosol, only to be reimported back into the nucleus (30). This reinfection cycle may in part explain the chronic nature of infection.

Taken together, the data confirm that M1 is the main factor responsible for determining the directionality of vRNP transport. When vRNPs are associated with M1, they are unable to enter the nucleus; when M1 is off, they can enter. M1 can undergo an low-pH-triggered change which leads, at least under the conditions prevailing in the cytosol, to its dissociation from vRNPs. In the incoming virus, the change is normally mediated by M2 and induced by the low endosomal pH. Whether additional cytosolic modifications such as phosphorylation or zinc binding are involved in releasing the acid-exposed M1 molecules remains to be determined (7).

Every specific contact between viral components provides a potential target for antiviral interference. That expression of a structural protein, M1, protects a mammalian cell against infection can be exploited to generate cells and organisms that are refractory to the virus. This illustrates the emerging concept that viral proteins may effectively be used as specific weapons against virus infection. This approach has already resulted in the engineering and development of virus-resistant crops (55). It could, in the future, be applied to animal systems as well.

ACKNOWLEDGMENTS

We thank Robert Krug for providing the virus stocks, Peter Palese for the M1 constructs, Henrik Garoff for the SFV plasmids, Mark Krystal for the 3PNP-4 cell line, Sandra Wolin for the L929 cell line, Mark Bevensee for advice on cytosol acidification, and Martina Ittensohn for help with hybridomas. We also thank Jani Simons, Päivi M. Ojala, Urs Greber, Beate Sodeik, and Dan Hebert for critical reading of the manuscript.

M.B. was supported by fellowships from the Life and Health Insurance Medical Research Fund and the National Institutes of Health (MSTP training grant GM 07205), and G.W. was supported by a long-term fellowship from the European Molecular Biology Organization and a Brown-Coxe fellowship. The support of the National Institutes of Health (grant AI 18599) is also acknowledged.

REFERENCES

1. **Boron, W. F.** 1977. Intracellular pH transients in giant barnacle muscle fibers. Am. J. Physiol. **233:**C61–C71.
2. **Bukrinskaya, A. G., N. K. Vorkunova, G. V. Kornilayeva, R. A. Narmanatova, and G. K. Vorkunova.** 1982. Influenza virus uncoating in infected cells and effect of rimantadine. J. Gen. Virol. **60:**49–59.
3. **Compans, R. W., J. Content, and P. H. Duesberg.** 1972. Structure of the ribonucleoprotein of influenza virus. J. Virol. **10:**795–800.
4. **Davey, J., N. J. Dimmock, and A. Colman.** 1985. Identification of the sequences responsible for the nuclear accumulation of the influenza virus nucleoprotein in Xenopus oocytes. Cell **40:**667–675.
5. **Davidson, R. L., and P. S. Gerald.** 1976. Improved methods for the induction of mammalian cell hybridization by polyethylene glycol. Somatic Cell Genet. **2:**165–176.
6. **Duesberg, P. H.** 1969. Distinct subunits of the ribonucleoprotein of influenza virus. J. Mol. Biol. **42:**485–499.

7. **Elster, C., E. Fourest, F. Baudin, K. Larsen, S. Cusak, and R. Ruigrok.** 1994. A small percentage of influenza virus M1 protein contains zinc but zinc does not influence in vitro M1-RNA interaction. J. Gen. Virol. **75:**37–42.
8. **Guinea, R., and L. Carrasco.** 1995. Requirement for vacuolar proton-ATPase activity during entry of influenza virus into cells. J. Virol. **69:**2306–2312.
9. **Hauser, J.** 1989. Effects of cytoplasmic acidification on clathrin lattice morphology. J. Cell Biol. **108:**401–411.
10. **Hay, A. J.** 1989. The mechanism of action of amantadine and rimantadine against influenza viruses, p. 361–367. *In* A. L. Notkins and M. B. A. Oldstone (ed.), Concepts in viral pathogenesis III. Springer Verlag, New York.
11. **Hay, A. J., A. J. Wolstenholme, J. J. Skehel, and M. H. Smith.** 1985. The molecular basis of the specific anti-influenza action of amantadine. EMBO J. **4:**3021–3024.
12. **Helenius, A.** 1992. Unpacking the incoming influenza virus. Cell **69:**577–578.
13. **Jennings, P. A., J. T. Finch, G. Winter, and J. S. Robertson.** 1983. Does the higher order structure of the influenza virus ribonucleoprotein guide sequence rearrangements in influenza viral RNA? Cell **34:**619–627.
14. **Kann, M., X. Lu, and W. H. Gerlich.** 1995. Recent studies on replication of hepatitis B virus. J. Hepatol. **22:**9–13.
15. **Kato, N., and H. J. Eggers.** 1969. Inhibition of uncoating of fowl plague virus by amantadine hydrochloride. Virology **37:**632–641.
16. **Kemler, I., G. Whittaker, and A. Helenius.** 1994. Nuclear import of microinjected influenza virus ribonucleoproteins. Virology **202:**1028–1033.
17. **Koff, W. C., and V. Knight.** 1979. Inhibition of influenza virus uncoating by rimantadine hydrochloride. J. Virol. **31:**261–263.
18. **Lamb, R. A.** 1989. Genes and proteins of the influenza viruses, p. 1–87. *In* R. M. Krug (ed.), The influenza viruses. Plenum Press, New York.
19. **Lamb, R. A., S. L. Zebedee, and C. D. Richardson.** 1985. Influenza virus M2 protein is an integral membrane protein expressed on the infected-cell surface. Cell **40:**627–633.
20. **Li, R., P. Palese, and M. Krystal.** 1989. Complementation and analysis of an NP mutant of influenza virus. Virus Res. **12:**97–112.
21. **Li, R., and J. O. Thomas.** 1989. Identification of a human protein that interacts with nuclear localization signals. J. Cell Biol. **109:**2623–2632.
22. **Liljestrom, P., and H. Garoff.** 1991. A new generation of animal cell expression vectors based on the Semliki Forest virus replicon. Bio/Technology **9:**1956–1963.
23. **Maeda, T., K. Kawasaki, and S. Ohnishi.** 1981. Interaction of influenza virus hemagglutinin with target membrane lipids is a key step in virus-induced hemolysis and fusion a pH 5.2. Proc. Natl. Acad. Sci. USA **78:**4133–4137.
24. **Marsh, M., and A. Helenius.** 1989. Virus entry into animal cells. Adv. Virus Res. **36:**107–151.
25. **Martin, K., and A. Helenius.** 1991. Nuclear transport of influenza virus ribonucleoproteins: the viral matrix protein (M1) promotes export and inhibits import. Cell **67:**117–130.
26. **Martin, K., and A. Helenius.** 1991. Transport of incoming influenza virus nucleocapsids into the nucleus. J. Virol. **65:**232–244.
27. **Martin, K., I. Kemler, and A. Helenius.** 1992. Inhibitory action of amantidine during influenza virus entry: a hypothesis, p. 183–190. *In* T. K. Korhonen (ed.), Molecular recognition in host-parasite interactions. Plenum Press, New York.
28. **Matlin, K. S., H. Reggio, A. Helenius, and K. Simons.** 1982. Infectious entry pathway of influenza virus in a canine kidney cell line. J. Cell Biol. **91:**601–613.
29. **Murti, K. G., W. J. Bean, and R. G. Webster.** 1980. Helical ribonucleoproteins of influenza virus: an electron microscopic analysis. Virology **104:**224–229.
30. **Nassal, M., and H. Schaller.** 1993. Hepatitis B virus replication. Trends Microbiol. **1:**221–228.
31. **Okhuma, S., and B. Poole.** 1978. Fluorescence probe measurement of the intralysosomal pH in living cells and the perturbation of pH by various agents. Proc. Natl. Acad. Sci. USA **75:**3327–3331.
32. **O'Neill, R. E., R. Jaskunas, G. Blobel, P. Palese, and J. Moroianu.** 1995. Nuclear import of influenza virus RNA can be mediated by viral nucleoprotein and transport factors required for protein import. J. Biol. Chem. **270:** 22701–22704.
33. **O'Neill, R. E., and P. Palese.** 1995. NPI-1, the human homolog of SRP-1, interacts with influenza virus nucleoprotein. Virology **206:**116–125.
34. **Patterson, S., J. Gross, and J. S. Oxford.** 1988. The intracellular distribution of influenza virus matrix protein and nucleoprotein in infected cells and their relationship to haemagglutinin in the plasma membrane. J. Gen. Virol. **69:**1859–1872.
35. **Pinto, L. H., L. J. Holsinger, and R. A. Lamb.** 1992. Influenza virus M2 protein has ion channel activity. Cell **69:**517–528.
36. **Plotch, S. J., M. Bouloy, I. Ulmanen, and R. M. Krug.** 1981. A unique cap (m7GpppXM)-dependent influenza virion endonuclease cleaves capped RNAs to generate primers that initiate viral RNA transcription. Cell **23:**847–858.
37. **Rees, P. J., and N. J. Dimmock.** 1981. Electrophoretic separation of influenza virus ribonucleoproteins. J. Gen. Virol. **53:**125–132.
38. **Rink, T. J., R. Y. Tsien, and T. Pozzan.** 1982. Cytoplasmic pH and free Mg^{2+} in lymphocytes. J. Cell Biol. **95:**189–196.
39. **Rochanovsky, O. M.** 1976. RNA synthesis by ribonucleoprotein-polymerase complexes isolated from influenza virions. Virology **73:**327–338.
40. **Sandvig, K., S. Olsnes, O. W. Petersen, and B. van Deurs.** 1987. Acidification of the cytosol inhibits endocytosis from coated pits. J. Cell Biol. **105:**679–689.
41. **Schroeder, C., C. M. Ford, S. A. Wharton, and A. J. Hay.** 1994. Functional reconstitution in lipid vesicles of influenza virus M2 protein expressed by baculovirus: evidence for proton transfer activity. J. Gen. Virol. **75:**3477–3484.
42. **Schulze, I. T.** 1970. The structure of influenza virus. I. The polypeptides of the virion. Virology **42:**890–904.
43. **Shimbo, K., D. L. Brassard, R. A. Lamb, and L. H. Pinto.** 1996. Ion selectivity and activation of the M_2 ion channel of influenza virus. Biophys. J. **70:**1335–1346.
44. **Singh, I., and A. Helenius.** 1992. Role of ribosomes in Semliki Forest virus nucleocapsid uncoating. J. Virol. **66:**7049–7058.
45. **Skehel, J. J.** 1992. Amantadine blocks the channel. Nature (London) **358:** 110–111.
46. **Sugrue, R. J., G. Bahadur, M. C. Zambon, S. M. Hall, A. R. Douglas, and A. J. Hay.** 1990. Specific structural alteration of the influenza haemagglutinin by amantadine. EMBO J. **9:**3469–3476.
47. **Sugrue, R. J., and A. J. Hay.** 1991. Structural characteristics of the M2 protein of influenza A viruses: evidence that it forms a tetrameric channel. Virology **180:**617–624.
48. **Wakefield, L., and G. G. Brownlee.** 1989. RNA-binding properties of influenza A virus matrix protein M1. Nucleic Acids Res. **17:**8569–8580.
49. **Wang, C., R. A. Lamb, and L. H. Pinto.** 1994. Direct measurement of the influenza A virus M2 protein ion channel activity in mammalian cells. Virology **205:**133–140.
50. **Wang, C., K. Takeuchi, L. H. Pinto, and R. A. Lamb.** 1993. Ion channel activity of influenza A virus M2 protein: characterization of the amantadine block. J. Virol. **67:**5585–5594.
51. **Wharton, S. A., A. J. Hay, R. J. Sugrue, J. J. Skehel, W. I. Weis, and D. C. Wiley.** 1990. Membrane fusion by influenza viruses and the mechanism of action of amantadine, p. 1–12. *In* W. G. Laver and G. M. Air (ed.), Use of X-ray crystallography in the design of antiviral agents. Academic Press, Inc., Orlando, Fla.
52. **White, J., J. Kartenbeck, and A. Helenius.** 1982. Membrane fusion activity of influenza virus. EMBO J. **1:**217–222.
53. **Whittaker, G., M. Bui, and A. Helenius.** 1996. Nuclear trafficking of influenza A virus ribonucleoproteins in heterokaryons. J. Virol. **70:**2743–2756.
54. **Whittaker, G., M. Bui, and A. Helenius.** 1996. The role of nuclear import and export in influenza virus infection. Trends Cell Biol. **6:**67–73.
55. **Wu, X. J., R. N. Beachy, T. M. Wilson, and J. G. Shaw.** 1990. Inhibition of uncoating of tobacco mosaic virus particles in protoplasts from transgenic tobacco plants that express the viral coat protein. Virology **179:**893–895.
56. **Ye, Z. P., R. Pal, J. W. Fox, and R. R. Wagner.** 1987. Functional and antigenic domains of the matrix (M1) protein of influenza A virus. J. Virol. **61:**239–246.
57. **Zhirnov, O. P.** 1992. Isolation of matrix protein M1 from influenza viruses by acid-dependent extraction with nonionic detergent. Virology **186:**324–330.
58. **Zhirnov, O. P.** 1990. Solubilization of matrix protein M1/M from virions occurs at different pH for orthomyxo- and paramyxoviruses. Virology **176:** 274–279.
59. **Zvonarjev, A. Y., and Y. Z. Ghendon.** 1980. Influence of membrane (M) protein on influenza A virus virion transcriptase activity in vitro and its susceptibility to rimantadine. J. Virol. **33:**583–586.